High-resolution global map of smallholder and industrial closed-canopy oil palm plantations

Adrià Descals[1], Serge Wich[2,3], Erik Meijaard[4,5,6], David L.A. Gaveau[7,8], Stephen Peedell[9], and Zoltan Szantoi[9,10,*]

[1]CREAF, Cerdanyola del Vallès, 08193 Barcelona, Spain; a.descals@creaf.uab.cat
[2]School of Biological and Environmental Sciences, Liverpool John Moores University, James Parsons Building, Byrom, Street, Liverpool L3 3AF, UK; S.A.Wich@ljmu.ac.uk
[3]Institute for Biodiversity and Ecosystem Dynamics, University of Amsterdam, Science Park, 904, 1098 XH, Amsterdam, The Netherlands
[4]Borneo Futures, Bandar Seri Begawan BA 2711, Brunei Darussalam; emeijaard@gmail.com
[5]Durrell Institute of Conservation and Ecology, University of Kent, Canterbury CT2 7NR, UK
[6]School of Biological Sciences, University of Queensland, Queensland 4072, Australia
[7]Center for International Forestry Research, P.O. Box 0113 BOCBD, Bogor, Indonesia; d.gaveau@cgiar.org
[8]TheTreeMap, Bagadou Bas 46600 Martel, France
[9]European Commission, Joint Research Centre, 20127 Ispra, Italy; stephen.peedell@ec.europa.eu
[10]Stellenbosch University, Stellenbosch 7602, South Africa

Correspondence to: Zoltan Szantoi (zoltan.szantoi@ec.europa.eu)

Abstract. Oil seed crops, especially oil palm, are among the most rapidly expanding agricultural land uses, and their expansion is known to cause significant environmental damage. Accordingly, these crops often feature in public and policy debates, which are hampered or biased by a lack of accurate information on environmental impacts. In particular, the lack of accurate global crop maps remains a concern. Recent advances in machine learning and remotely-sensed data access make it possible to address this gap. We present an up-to-date map of closed-canopy oil palm (*Elaeis guineensis*) plantations by typology (industrial vs. smallholder plantations) at the global scale and with an unprecedented detail (10-meter resolution). Sentinel-1 and Sentinel-2 data were used to train a DeepLabv3+ model, a convolutional neural network (CNN) for semantic segmentation. The characteristic backscatter response of closed-canopy oil palm stands in Sentinel-1 and the ability of CNN to learn the spatial patterns, such as the harvest road networks, allowed the distinction between industrial and smallholder plantations globally (overall accuracy = 97.5% and kappa = 84.9%). The user's accuracy in industrial and smallholders was 73.8% and 89.4%, and the producer's accuracy was 85.6% and 78.8% respectively. The global oil palm layer reveals that oil palm plantations are found in 47 tropical countries. Southeast Asia ranks as the main producing region with 17.47 x 10^6 ha, or 90% of global plantations. Our analysis confirms significant regional variation in the ratio of industrial versus smallholder growers, but also that, from a typical land development perspective, large areas of legally defined smallholder oil palm resemble industrial-scale plantings. The overall oil palm surface per country is similar to the harvested area reported by FAO, except for countries in Western Africa, where our estimates are lower due to the omission of feral oil palm plantations. In Indonesia, the world's largest producer, our planted area estimate is higher because FAO does not report unregistered landholdings. Our model identifies primarily closed-canopy oil palm stands and misses young or sparsely planted oil palm

Open Access

Earth System
Science
Data

Discussions

stands. An accurate global map of planted oil palm can help to shape the ongoing debate about the environmental impacts of oil seed crop expansion, especially if other crops can be mapped to the same level of accuracy. As our model can be regularly rerun as new imagery is published, it can be used to reliably to monitor the expansion of a crop. The global oil palm layer for the second half of the year 2019 at a spatial resolution of 10 meters can be found at

40   https://doi.org/10.5281/zenodo.3884602 (Descals et al., 2020).

1 Introduction

Crops that produce vegetable oils, such as soy, rapeseed, oil palm, and sunflower, take up ca. 6% of all agricultural land and ca. 2.3% of the total global land area, and are among the world's most rapidly expanding crop types (OECD, 2018). Demand for vegetable oils is increasing, with one estimate foreseeing an increase from 205 Mt in 2019 (OECD, 2018) to 310 Mt in

45   2050 (Byerlee et al., 2017). This has created a need to optimize land use for vegetable oil production in order to minimize environmental impacts and maximize socio-economic benefits. One of the requirements for this is accurate global maps for all oil-producing crops. The most comprehensive maps available (IFPRI, 2019) map these crops by disaggregating crop statistics identified at national and sub-national units for the year 2005 to 5 arc-minute grid cells, which is a relatively coarse spatial resolution. Direct identification of crops from satellite imagery is likely to result in more accurate maps that delineate

50   where different crops have been planted. One of the most extensively mapped crops is oil palm (Elaeis guineensis) because of societal concerns about the associated environmental impacts on tropical forests and social disruption. However, only the global extent of industrial plantations is reasonably well known, while the more heterogeneous plantings at smallholder scales remain largely unmapped (Meijaard et al., 2018).

A global map of oil palm at each production scale provides critical insights to the current debate about the social and

55   environmental sustainability of the crop (Meijaard et al., 2018). It would allow for a more accurate determination of the environmental impacts from oil palm expansion, for example, by assessing the deforestation that preceded oil palm development, the related carbon emissions as well as the impacts on species' distributions, key biodiversity areas, and socio-economic impacts. As total and local production volumes of palm oil are reasonably well known, a comparison to the total planted area would allow more accurate average yield estimates and regional variations in yield. Similarly, accurate maps of

60   planted oil palm can determine the extent to which oil palm development has displaced other food crops, an important element in the policy debate in the European Union regarding the use of palm oil in biofuels (Meijaard & Sheil, 2019). Such information is important for comparing oil palm to other vegetable oil crops, such as soy, rapeseed, sunflower, groundnut, and coconut, once global maps for these crops become available. The challenge is thus to develop a method to accurately map large industrial plantations as well as smallholder oil palm areas.

65   Previous studies have demonstrated the usefulness of radar imagery for the detection of closed-canopy oil palm stands. Palm-like trees have a characteristic backscatter response which consists of a high vertical transmit and vertical receive (VV)

and lower horizontal transmit and vertical receive (HV) in Sentinel-1, or a high horizontal transmit and vertical receive (HV) and low horizontal transmit and horizontal receive (HH) in PALSAR imagery (Miettinen & Liew, 2011). This characteristic backscatter response is a consequence of the canopy structure of palm-like trees and allows the detection of closed-canopy

70   palm plantations, particularly oil palm. Several studies have taken advantage of this characteristic backscatter response for mapping oil palm at the local and the regional scale (Koh et al., 2011; Lee et al., 2016; Nomura et al., 2019; Oon et al., 2019), and similarly using supervised classification models (Descals et al., 2019; Shaharum et al., 2020; Xu et al., 2020).

The mapping of oil palm plantations by typology (smallholder versus industrial) with remotely-sensed data presents a more challenging classification problem than the detection of only closed-canopy oil palm. In addition to the backscatter response

75   of radar data, texture analysis also offers a complimentary method to identify distinctions between smallholders and industrial-scale plantations (Descals et al., 2019). Contextual information observes spatial patterns such as the road network in plantations, drainage structure, and association with palm oil mills, which can help to distinguish between industrial and smallholder plantations.

Deep learning, in particular semantic segmentation, is a subfield of machine learning with characteristics suitable for the

80   distinction of smallholder and industrial oil palm plantations. Deep learning employs a series of models for computer vision that excel in very complex classification scenarios (LeCun et al., 2015) and, in particular, convolutional neural networks (CNN) have recently been embraced by the remote sensing community due to the ability to recognize intricate patterns in the images (Ma et al., 2019). To date, there are no studies that consider CNN for the land use classification of oil palm plantations at regional or global scales. Only a few studies use deep learning for object detection, and have only achieved the

85   identification of single palm trees (Li et al., 2017).

The aim of this study is i) present an up-to-date map of oil palm plantations by typology (industrial vs. smallholder plantations) at the global scale and with unprecedented detail (10-meter resolution) for the year 2019 and ii) show the suitability of deep learning in remote sensing for complex classification scenarios in which contextual information may be useful.

90   **2 Methods**

2.1 Overview

The classification model for oil palm plantations uses the Sentinel-1 and Sentinel-2 half-yearly composites as input images (Figure 1). The maps presented in this study correspond to the second half-year of 2019. The deep learning model that we used is the DeepLabv3+ (Chen et al., 2018) based on MobileNetV2 (Sandler et al., 2018) as the CNN backbone. The model

95   was trained with 296 images of 1000x1000 pixels distributed throughout the main oil palm producing regions and applied over Sentinel-1 and Sentinel-2 composites in the potential area (Figure 2) where oil palm can grow.

Earth System
Science
Data

Open Access

Discussions
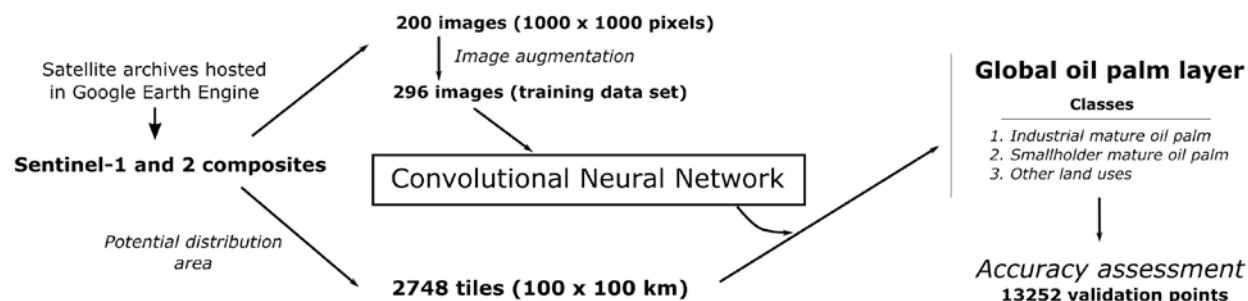
Figure 1: Diagram of the algorithm used to generate the global oil palm layer. The input images, Sentinel-1 and Sentinel-2 half-year composites, were obtained from Google Earth Engine in a grid of 100 x 100 km. The Sentinel-1 and Sentinel-2 tiles were
100 **classified with a convolutional neural network (CNN). The CNN model was trained with labeled images with constant size (1000 x 1000 pixels). The output classification layer was validated with 13,252 points that were randomly distributed.**

2.2 Potential distribution of oil palm

The classification of land cover for oil palm plantations was restricted to those areas where the climatic conditions are favorable for oil palm growth. In order to delimit the potential distribution of oil palm, we used climate data and an existing

105 global oil palm dataset. The climate dataset was obtained from WorldClim V1 Bioclim (Hijmans et al., 2005), which provides nineteen gridded variables at a spatial resolution of 30 arc seconds that are generated from monthly temperature and precipitation. This study's existing oil palm layer was obtained from the IUCN (Meijaard et al., 2018) and shows the industrial oil palm plantations at the global scale. This map was derived from a compilation of all published spatial data on oil palm combined with manual digitizing of characteristics spatial signatures of industrial-scale oil palm using cloud-free

110 Landsat mosaics acquired in 2017, created in Google Earth Engine (GEE).

The potential area where oil palm can grow was estimated with the climate variable range in the IUCN layer. We estimated the histogram of the nineteen bioclimatic variables in the areas that are classified as industrial oil palm plantations in the IUCN layer. Supplementary to this, Table 1 shows the minimum and maximum of each bioclimatic variable for the industrial plantations. A pixel in the WorldClim dataset was considered favorable for oil palm growth when at least seventeen out of

115 the nineteen bioclimatic variables fell within the climate range observed in the IUCN layer (Supplementary figure 1). The resulting potential oil palm distribution map encompasses similar areas as used in previous studies (Pirker et al., 2016; Strona et al., 2018; Wich et al., 2014). The classification of oil palm plantations was processed in a grid of 100 x 100 kilometers that covers the area with favorable conditions for oil palm growth (Figure 2).
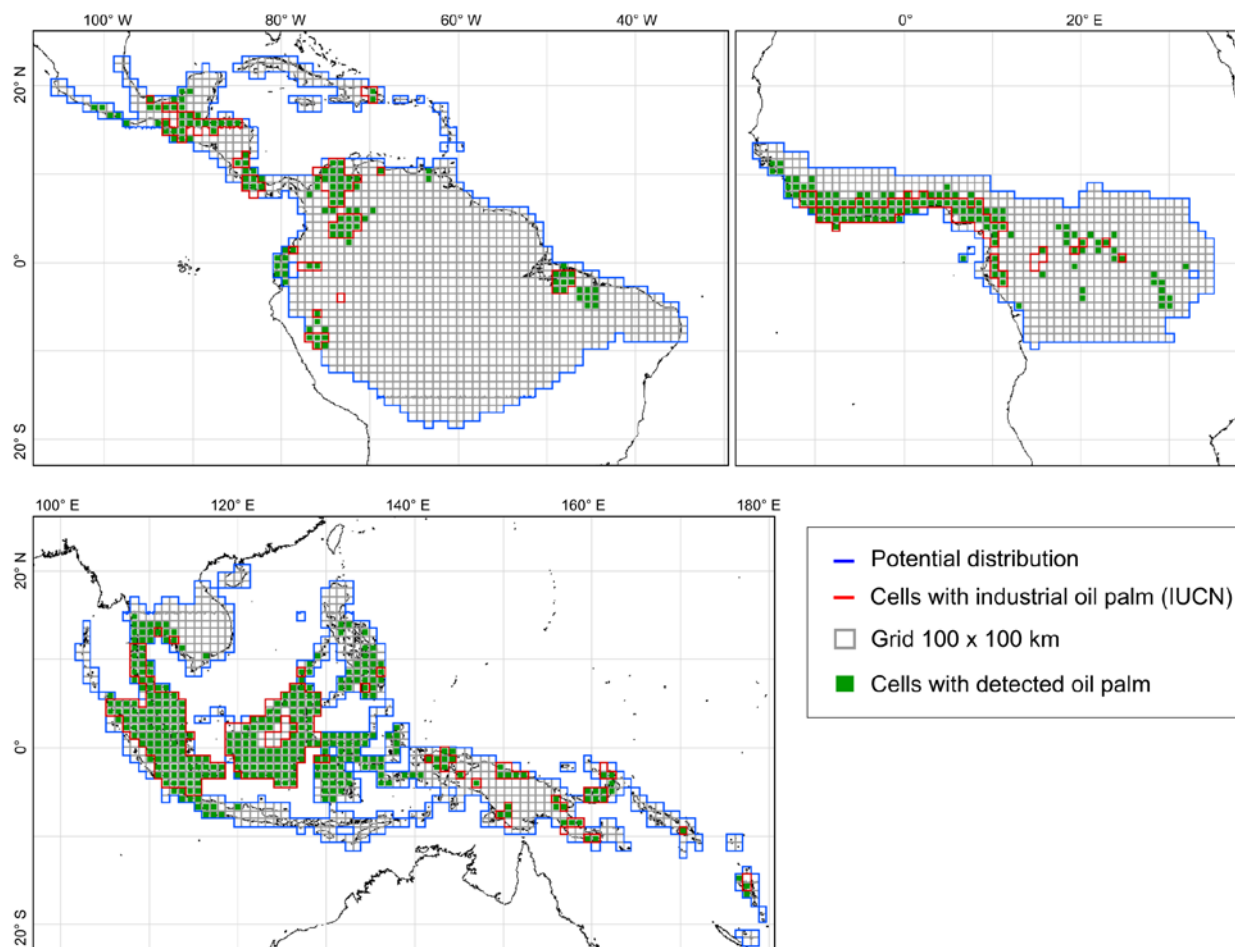
Figure 2: Localization map of the grid cells where the Convolutional Neural Network was applied for the classification of industrial and smallholder plantations. The grid cells cover a potential distribution area (blue line) over 6 tropical regions of the world where oil palm can grow: Southeast Asia, Central and South America, Central and Western Africa and the Pacific. Cells in red depict the areas where there is presence of industrial oil palm plantations in the IUCN layer. Cells filled with green signifiy areas where oil palm was detected with the convolutional neural network.

2.3 Sentinel-1 and Sentinel-2 pre-processing

The CNN classifies radar and spectral images collected by Sentinel-1 (C-band) and Sentinel-2 (multispectral) satellites, both missions launched by the European Space Agency and part of the Copernicus Programme (www.copernicus.eu). The images were pre-processed and downloaded from GEE. We used the Sentinel-1 SAR Ground Range Detected (GRD) in both ascending and descending orbits at a spatial resolution of 10 meters. The scenes were processed with the local incident angle (LIA) correction and then the median value was computed over the second half-year of 2019 for the ascending and

5

descending scenes separately. The final composite is the average of the two orbit composites (more information in section 5. Code availability).

We also used Band 4 (red band) of Sentinel-2 Level 2A (top-of-atmosphere reflectances). Different feature selection algorithms highlighted the relevance of Band 4 for predicting industrial and oil palm plantations in a previous study (Descals

135　et al., 2019). Band 4 is the 10-meter resolution band that best shows the roads in industrial plantations because of the high contrast in terms of reflectance between the road and the surrounding oil palm. The high light scattering of vegetation in the near-infrared spectrum makes the recognition of roads less feasible in the 10-meter near-infrared band (B8). The Sentinel-2 images were masked with the quality flag provided in the Level 2A, which provides information about the clouds, cloud shadows, and other non-valid observations. The images were aggregated for the second half-year of 2019 using the

140　normalized difference vegetation index as the quality mosaic (more information in section 5. Code availability).

2.4 Image labelling

Semantic segmentation models require input images with a constant size for both training and prediction. The size of the input images in this study was set to 1000 x 1000 pixels, which corresponds to an area of 10 x 10 km in a 10-meter-resolution image. We set an input size of 10 km because it captures the contextual spatial information necessary for

145　identifying smallholders and industrial plantations (e.g., roads, mills). Consequently, the model was trained with Sentinel-1 and Sentinel-2 half-yearly annual composites of the size of 10 x 10 km that were labeled by visual interpretation of the high-resolution images that are provided by DigitalGlobe and used as a base layer in Google Earth. We used the geometry editing tool in GEE for labeling smallholder and industrial plantations and for downloading the labeled images along with the Sentinel-1 and Sentinel-2 composites for the second half-year of 2019. The image labeling was carried out in 84 different

150　regions of the world where oil palm is cultivated (Supplementary figure 2) and resulted in 200 training images.

Deep learning algorithms require large amounts of data to ensure good performance and image augmentation is a technique that is often used to improve the performance of the models when the size of the training data is small. We used the rotation of images (90 degrees clockwise) as the data augmentation technique for this study (Supplementary figure 3). The rotation was applied only to the training images that presented more than 10% of the pixels labeled as smallholders in order to reduce

155　the class imbalance between industrial and smallholder plantations. We also clipped the central area of 4x4 blocks of labelled images and rotated them with an angle of 45°. This process resulted in 96 additional images that were added to the 200 original training images.

2.5 Definition of industrial and smallholder plantations

Definitions of smallholders and industrial plantations differ per country, and many variations within each of these classes

160　exist (Bronkhorst et al., 2017; Glenday & Gary, 2015; Erik Meijaard & Sheil, 2019). For the purposes of the current study,

we use the following generalized classifications. An *industrial oil palm* plantation typically covers several thousand hectares of land and is very well structured and homogeneous in tree age. It consists of an area bounded by long linear, sometimes rectangular boundaries. It has a dense trail and a road/canal network. Roads in industrial plantations are developed at the start of plantation and, therefore, equidistantly placed for optimal harvesting. In flat surface plantations, the harvesting trails

165 are usually built in straight lines and thus form a rectilinear grid (Figure 3a). In contrast, the industrial plantations that are constructed over steep terrain usually present curvy trails (Figure 3b). A *smallholder oil palm plantation* must be typically smaller than 25 ha to be recognized as 'small' by the Indonesian government. These definitions vary by country with Malaysia using a 4 ha cut-off, while in Cameroon this varies from 8 to 40 ha (for an overview, see Meijaard et al. 2018, Table 2). Compared to an industrial plantation, smallholder plantation tends to be less structured in shape and more

170 heterogeneous in tree age. Smallholder plantations tend to form a landscape mosaic, composed of small plantations of varying shape and size, mixed with other types of land cover (e.g., idle land or other plantation types) (Figure 3d). When smallholder plantations form a large homogenous cluster, this cluster has a less dense trail network than industrial plantations (Figure 3a, c).
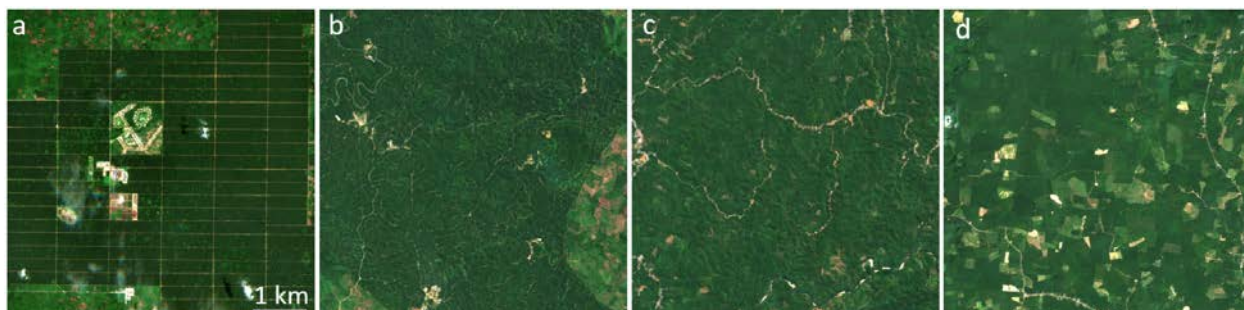
175 **Figure 3. Examples of industrial and smallholder oil palm plantations seen by Sentinel-2 imagery (10 m spatial resolution) displayed in true colors. Here, closed-canopy oil palm appears dark green, open-canopy oil palm has different shades of green. a) An industrial plantation on a flat surface in Nigeria, with harvesting trails built in straight lines and thus forming rectilinear grids. b) An industrial plantation on hilly terrain in Indonesia, with curvy harvesting trails. c) Smallholder plantations forming a large homogeneous cluster in Indonesia. d) Smallholder plantations of varying shapes, size, and tree age in Southern Thailand.**

180 **2.6 Semantic segmentation**

Image segmentation is the subfield of deep learning that aims to link each pixel of an image to a class label. Thus, semantic segmentation is the analog of the standard pixel-wise machine learning algorithms that are used in remote sensing for image classification (Ma et al., 2019). The difference is that semantic segmentation, as any model based on CNN, automatically learns and exploits the spatial patterns within the image by tuning the parameters of different convolutional operations. For

185 instance, CNN can automatically learn contextual information such as the road network in industrial plantations or the heterogeneity in landscape mosaics of smallholders.

This study emloyed the classification model DeepLabv3+ (Chen et al., 2018) with the MobileNetV2 (Sandler et al., 2018) as a backbone network. DeepLab has a series of versions for semantic segmentation. DeepLabv3+ is the latest version. The model uses an encoder-decoder architecture, in which the image is downsampled with max-pooling layers during the

190 encoder part and spatial information is retrieved during the decoder part. A characteristic of DeepLabv3+ is that the CNN uses atrous convolutions, which enhances the field of view of the image convolutions. The second-last layer of the CNN shows the probability that a pixel belongs to a certain class and the last operation of the CNN assigns the class with the maximum value in the probability layers, resulting in the final classification layer.

2.7 Validation

195 The validation of the global classification layer was performed with 13,252 points; 865 points were industrial plantations, 355 were smallholders, and 12,058 were other types of land uses (class 'Other'). Since the study aims to classify closed-canopy oil palm against other land uses, we included young oil palm and plantations that have not reached the full canopy coverage in the class 'Other'. The points were randomly distributed and visually interpreted with high-resolution images and with Sentinel-1 and Sentinel-2 composites. 11,570 points were randomly distributed in the 100 x 100 km cells where the

200 IUCN showed the presence of industrial plantations. The amount of grid cells with industrial plantations is 384 (Figure 2), 80 in America, 67 in Africa, and 237 in Southeast Asia and Pacific. The remaining 1,682 points were randomly distributed in a buffering area of 5 km around the industrial plantations of the IUCN layer. Similarly to the image labeling, we used Sentinel-1 and 2 composites and the high-resolution images in Google Earth for the visual interpretation of the points.

3 Results

205 The global map of industrial and smallholder plantations reveals the importance of high-resolution images (10 meters) for the accurate delimitation of smallholder plantations. Figure 4 shows the degree of detail of the classification image obtained with Sentinel-1 and Sentinel-2 composites. The figure also exemplifies the classification of industrial plantations, with the characteristic road network and the surrounding smallholder plantations. Supplementary Figure 4 shows examples of landscape types of oil palm plantations that were successfully detected and others that were omitted.
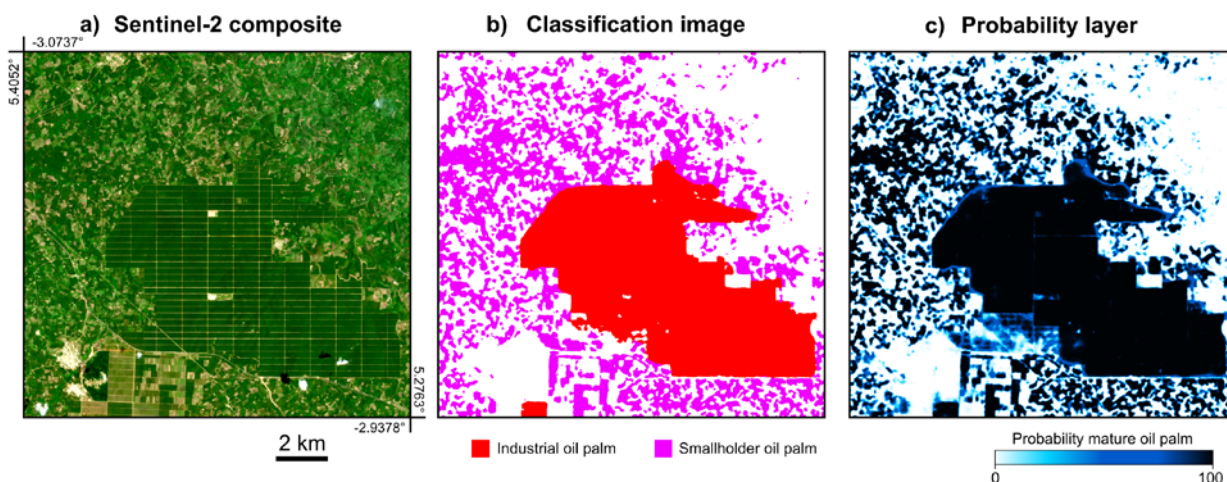
Figure 4. Example of the global oil palm layer in Cote d'Ivoire. Panel a) shows a Sentinel-2 true color composite. Panel b) shows the resulting classification image obtained with a convolutional neural network (CNN). The classification image depicts an industrial plantation (red) surrounded by smallholder plantations (purple). The CNN learns contextual information such as the rectilinear road network in the industrial plantation, which is noticeable in the Sentinel-2 composite. Panel c) shows the probability of closed-canopy oil palm. The probability layer was generated from the second last layer of the CNN, which reflects the probability of each class.

We estimated the global area of planted closed-canopy oil palm at 19.50×10^6 ha, of which 13.10×10^6 ha (67.2%) is industrial plantations and 6.40×10^6 ha (32.8%) is smallholders. The map confirms that Southeast Asia is the highest producing region in the world (Figure 5) with a total surface area of 17.47×10^6 ha. It is followed by South America (0.82×10^6 ha), Central America (0.49×10^6 ha), Western Africa (0.42×10^6 ha), Central Africa (0.16×10^6 ha), and the Pacific (0.14×10^6 ha). Oil palm plantations were found in 47 tropical countries (See Supplementary table 2). However, the estimated oil palm area varies greatly among countries, with Indonesia and Malaysia representing the bulk of the total surface area and with most of the countries with a plantation area below 2 ha $\times 10^6$ (Figure 6).
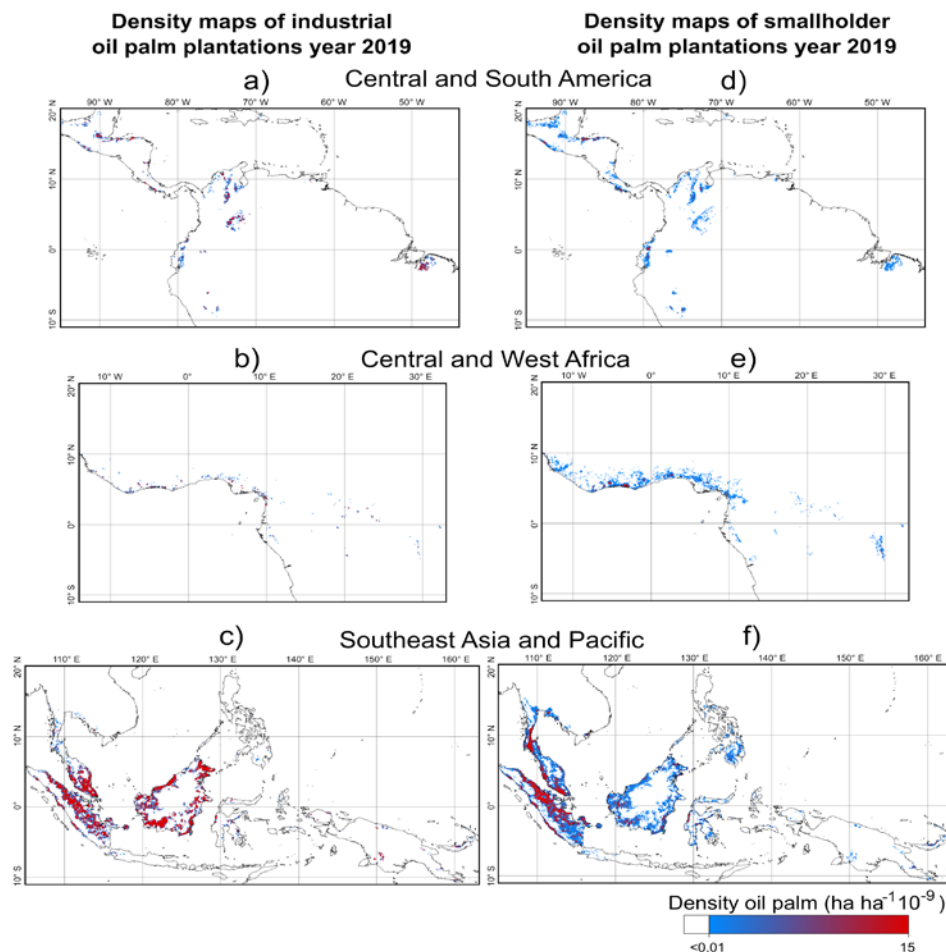
Figure 5. Density maps generated with the global oil palm layer. Panels a), b), and c) show the density maps of industrial oil palm plantations and panels d), e), and f) show the density maps for smallholder plantations. The maps have a spatial resolution of 10 km and represent the surface of closed-canopy oil palm, in hectares, in an area of 10^6 hectares. The values in the map were obtained by dividing the area of the oil palm within the 10-kilometer pixel by the total area covered in the pixel.

The region with the highest percentage of smallholder oil palm is West Africa (61.7 % of total plantings) (Supplementary figure 5). Elsewhere, the percentage of smallholders varies from 22.3% in South America to 36.5% in Central America. As Figure 6 illustrates, however, countries in the same region might show different proportions of smallholders and industrial plantations. For instance, Thailand shows the highest proportion of smallholders (95.1%) which differs from the low ratio in neighboring Malaysia (21.7%). Countries in Southeast Asia also show the highest oil palm surface per total land area (Supplementary figure 6), followed by smaller countries which allocate the majority of their cropland for oil palm production (Guatemala, Honduras, Costa Rica, and São Tomé and Príncipe).
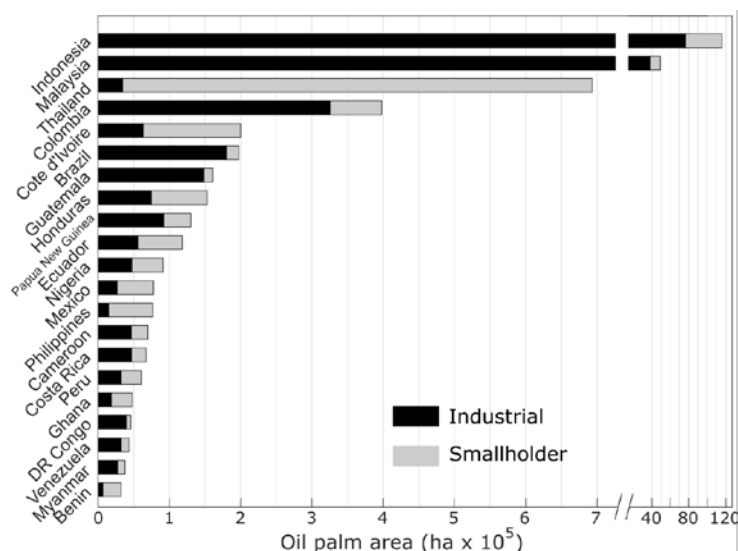
Figure 6. Oil palm plantation surface per country and typology for the second half-year of 2019. The area was estimated using the global oil palm layer that resulted from the classification of Sentinel-1 and Sentinel-2 composite at 10-meter resolution.

265 We evaluated the results of the CNN with 13,252 randomly distributed points and compared them with previous data sets in Sumatra for the year 2019 (Descals et al., 2019) and in Southeast Asia for the year 2016 (Xu et al., 2020). In order to compare the current results with the previous study (Descals et al., 2019), we kept only the validation points that cover Sumatra. This resulted in 2,463 points in total. For the comparison with Xu et al., 2020, we used our CNN model to classify Sentinel-1 and Sentinel-2 composites for the second half-year of 2016.

270

Table 1. Accuracy assessment of the global oil palm layer for the second half of 2019 and comparison of the global layer with the results of a previous study (Descals et al., 2019) in Sumatra for the same year. The accuracy metrics of the global layer were estimated with 13,252 points randomly distributed in the main oil palm producing areas in the world, while the comparison uses only the validation points that are located in Sumatra (2,463 points).

		Global OP	Global OP (Sumatra)	Descals et al., 2019
OA (%)		97.5	94.3	92.1
kappa		84.9	78.8	71.4
	Other	98.8	97.0	97.0
UA (%)	Industrial	89.4	89.3	88.7
	Smallholder	73.8	63.3	45.9
	Other	99.2	98.1	97.1
PA (%)	Industrial	78.8	71.5	58.8
	Smallholder	85.6	78.8	79.7

275

11

The accuracy metrics obtained with the 13,252 points show an OA of 97.5% and kappa of 84.9% (Table 1) for the global oil palm map. The high difference between the OA and kappa resulted from the high class imbalance in the validation dataset. Interestingly, the accuracy measures of Users (UA) and Producers (PA) show lower accuracies for industrial and smallholder plantations than the accuracies obtained for the class 'Other'. Smallholder plantations show the lowest UA (73.8%), while
280 the industrial plantations show the lowest PA (78.8%). Supplementary Table 3 shows the confusion matrix for the 13,252 points and reflects that the commission errors in smallholders were mostly misclassified from industrial plantations (65.7% of commission errors in smallholders belong to industrial plantations). Omission errors in industrial plantations were misclassified equally as 'Other' and smallholder plantations. The UA and PA accuracies are lower when evaluated only in Sumatra (smallholder UA = 63.3% and smallholder PA = 78.8%). However, these accuracies are considerably lower in
285 Descals et al., 2019, which presents a PA = 45.9 % for smallholders and UA = 58.8% for industrial plantations. Overall, the state-of-the-art methodology using CNN shows better accuracy metrics than the Random Forest classification for the case study in Sumatra, and also shows excellent results for the classification of global oil palm with UA and PA that are generally above 80%.

For the comparison with Xu et al. (2020), we reclassified the smallholders and industrial plantations as a single class. We
290 also removed the validation points that were placed in young plantations, and classified as 'Other', because the temporal analysis in Xu et al. (2020) also aims to detect young oil palm and the plantations that have been clear-cut in the previous years (Figure 7). Note that Xu's dataset includes a 100-meter multi-year classification and we only compared the last year (2016) to ensure data availability in Sentinel-1 over the study area. Our results (OA = 96.6% and kappa = 77.4%) performed better than Xu's classification image (OA = 92.2% and kappa = 61.2%) for 2016 (Supplementary Table 4). The omission
295 error in Xu's results (PA = 76.3%) are lower than our results (PA = 67.1%). However, the main difference between the data sets was found in the user's accuracy, in which our results excelled (UA = 96.6% compared to 57.4% in Xu's data set).
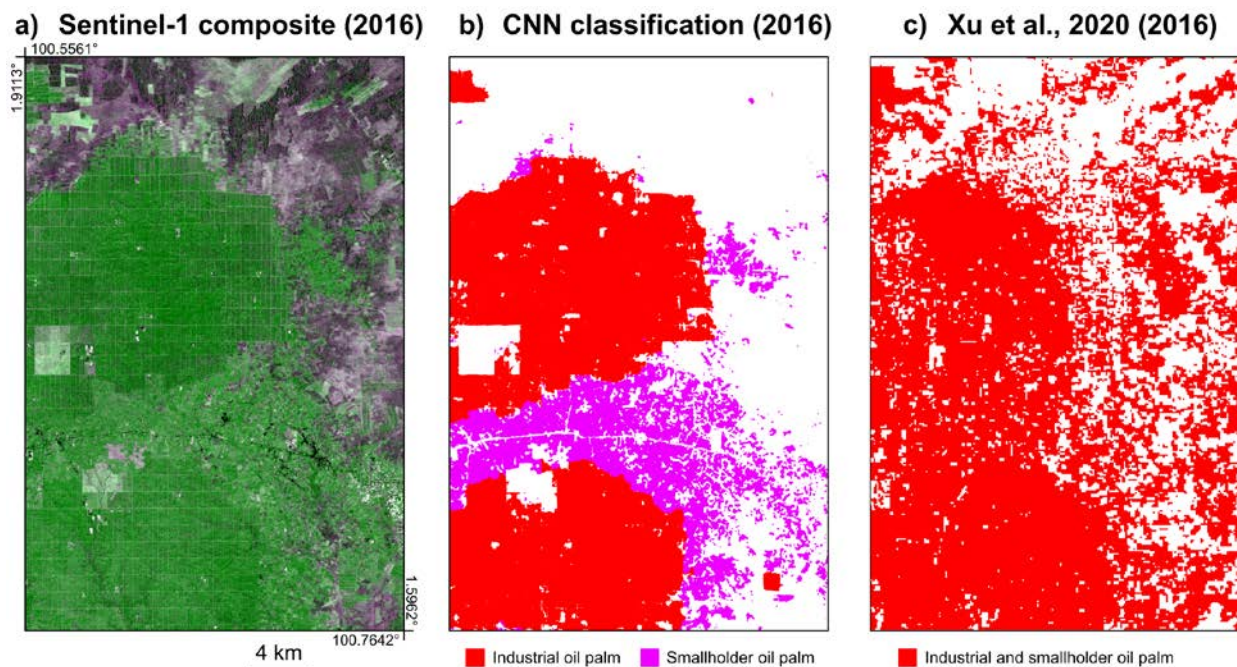
Figure 7. Comparison of the classification image obtained with the convolutional neural network (CNN) and the last year of the multiannual analysis presented in Xu et al., 2020. Panel a) shows a Sentinel-1 composite (VV-VH-VV) for the second half-year of
300 **2016 in Riau province (Indonesia). Panel b) shows the classification image that results from the CNN using the Sentinel-1 and Sentinel-2 composites for 2016. Panel c) shows the oil palm layer presented in Xu et al., 2020 for the year 2016.**

Comparison with Xu's data requires a degree of caution because it only reflects the accuracies for closed-canopy oil palm plantations, while the multi-annual analysis in Xu et al., 2020 aimed to detect disturbances in the time series in order to classify young plantations. This is also evidenced if we compare the global oil palm layer for 2019 with the data set in
305 Gaveau et al., (forthcoming), which maps oil palm and areas that have been clear-cut for oil palm plantation in Indonesia. We estimate that 11.54×10^6 ha of closed-canopy oil palm plantations existed in Indonesia in 2019, with 7.71×10^6 ha (66.8%) Industrial and 3.83×10^6 ha (33.2%) smallholder. By comparison, Gaveau et al. (forthcoming) found a higher oil palm area for Indonesia for the same year: 16.26×10^6 ha, but a similar ratio between industrial and smallholder plantation extent: 10.33×10^6 ha industrial (64%) and 5.93×10^6 ha smallholder (36%).

310 The comparison with inventories from FAOSTAT also evidences a large omission of oil palm plantations in West Africa (Supplementary figure 7). The total surface reported as harvested area in FAOSTAT is 4.16×10^6 ha in West Africa, while the total area estimated with the global oil palm layer is 0.42×10^6 ha. The country with the highest difference is Nigeria, with an area of 3.02×10^6 ha reported by FAOSTAT that contrasts with the 0.01×10^6 ha classified by the CNN. Our results also report more plantation area in Indonesia (11.54×10^6) than the reported by FAOSTAT (6.78×10^6). Overall, there is
315 high agreement between the CNN data and FAOSTAT data for other countries and the difference in oil palm area can be

Earth System
Science
Data

Open Access

Discussions

attributed to the different years used in the comparison; we used the last year of the FAOSTAT data (2018) while the global oil palm layer was generated for 2019.

4 Discussion

The results confirm previous findings on the suitability of radar satellite data for mapping closed-canopy oil palm plantations
320   at the regional scale (Miettinen & Liew, 2011). Our study further shows that these plantations can be mapped globally and by typology at high spatial resolution (10 meters). The results obtained with the CNN outperformed previous studies and provide evidence that deep learning is more suitable than standard machine learning algorithms, such as Random Forests, when contextual information is required for class prediction. Overall, the results show a high accuracy (Overall Accuracy = 97.5% and kappa = 84.9%). The accuracy assessment and the comparison with other products also evidences shortcomings
325   primarily in the classification of smallholder plantations, young plantations, plantations that have open canopies, and plantations mixed with non-palm tree species, such as semi-wild oil plantations in Africa.

Open-source deep learning libraries, such as TensorFlow or PyTorch, are democratizing deep learning to the broader scientific community. The model is planned to be used for follow-up monitoring once a year to generate global oil palm maps. The shortcomings of deep learning include the high computational cost for training the models and the high cost for
330   gathering labeled data. In this study, only 296 images of 1000 x 1000 pixels were used as a training data set, consisting of 200 labeled images and 96 augmented images. This quantity is far less than the thousands of training images often used in deep learning studies (i.e. more than 200,000 labeled images in the Common Objects in Context (COCO) dataset). In addition, databases with labeled data are scarce in remote sensing studies. Additional labeled data and pre-trained models would ease the computational cost of training CNN models in similar remote sensing studies.

335   We compared our findings with two studies, Xu et al. (2020) and Gaveau et al. (forthcoming). Our CNN model applied to Sentinel-1 and Sentinel-2 classified closed-canopy oil palm stands. Although, at coarser resolution (100m), the temporal analysis used in Xu et al., 2020 aimed to detect disturbances (e.g., land clearing and burning) which may or may not result in the development of oil palm plantations. Thus, Xu et al. classified opened-canopy plantations that remained undetected in our classification. Accordingly, the omission error was lower in Xu's case (PA = 76.3% vs PA = 67.1% in our estimate for
340   2016). However, Xu et al. detected much more than oil palm plantation, including scrubs and grasslands and, therefore, commission error was higher in Xu's map, UA = 57.4% compared to 96.6% in our classification.

Gaveau et al. (forthcoming) used a combination of Landsat and SPOT6 imagery to map oil palm plantations. They did not directly measure planted areas, but instead they identified areas that have been "cleared to develop plantations". An area may have been cleared for oil palm, left idle because of a number of constraints, or the area may have been planted but the
345   plantation may have failed. This evidences an important shortcoming with our method; the classification of oil palm with

radar data can only detect closed-canopy oil palm stands and, thus, excludes areas cleared for oil palm that have been left idle or where oil palm trees died. In addition, oil palm must be at least 3-years-old (Descals et al. 2019) to reach closed-canopy. Therefore, it is likely that our maps missed young smallholder oil palm plantations developed after 2016. Gaveau et al. is more suited to verify the impacts of the oil palm industry on forests, while our method is more suited to map the

350   productive planted area, i.e. closed-canopy oil palm stands > 3 years old.

Contextual to these insights, we note several caveats regarding our estimate of globally planted oil palm areas. We highlighted that our analysis generally does not detect young oil palm. In addition, our method also struggles to detect oil palm in non-homogeneous settings (e.g., oil palm mixed with other crops). This means that our global estimate of total planted oil palm areas is an underestimate. It is difficult to say by how much we underestimate the total planted area, but

355   assuming constant planting rates and an average age of 25 years of palms until replanting, we could miss 3/25 = 12% of the total planted area. Additionally, there are palms in agroforestry type settings that are difficult to quantify, primarily naturally occurring oil palm trees, known as feral oil palm, that are present in Africa. These semi-wild oil palm plantations explain the large difference with the harvested area reported by FAOSTAT in West Africa. Taking this into consideration, the global area of planted oil palm is likely to be 10-20% higher than our estimate (i.e., 21.5 - 23.4 x 10^6 ha).

360   Despite the caveats regarding the total areas of planted oil palm, our findings about the ratio between smallholders and industrial-type plantings are still relevant, as both types of oil palm are similarly affected by omission in our analysis (except the oil palm we miss in agroforestry type settings, which is mostly smallholders). An evidence of this is that the ratios reported by Gaveau et al. (forthcoming) are similar to our estimates in Indonesia. Globally, our data indicate that 67.2% of planted oil palm is under industrial-scale management and 32.8% managed by smallholders. These percentages diverge from

365   the commonly stated claim that 40% of the palm oil produced globally is from smallholders. Not only is the land managed in smallholder-type settings less than 40%, but there is also a significant yield gap between industrial-scale and smallholder-scale operators. Smallholder yields are often 40% or lower than yields in industrially-managed plantations (Woittiez et al., 2017), which suggests that the overall contribution of smallholders to global palm oil production is about 18% rather than 40%. Industrial-scale operators thus appear to produce about 82% of the global palm oil. We note that this excludes the

370   locally produced palm oil in agroforestry-type settings in the African tropics, where palm is traditionally produced for local consumption.

Our findings on the ratio between smallholder and industrial-scale oil palm are different from those reported by various governments. For example, the government of Indonesia estimates that 40.8% of the country's oil palm planted area is developed under smallholder licenses, whereas our analysis of the typical characteristics of planted crops indicate that this

375   ratio is 66.8% industrial and 33.2% smallholder for the country. To qualify as a 'smallholder farmer' in Indonesia, according to the government, farms must be less than 25 ha. Those that cultivate less than 25 ha of oil palm are required to apply for a Plantation Registration Certificate (STD-B), while those producers cultivating more than 25 ha require a Plantation Business

License (IUP-B) (Jelsma et al., 2017). The latter involves more complex procedures and regulatory requirements such as an environmental impact assessment (Paoli et al., 2013). Those with an STD-B are exempted from most of these requirements

380 (Jelsma et al. 2017). This creates an incentive for producers to classify their plantations as non-industrial scale because the paperwork and licensing involves fewer hurdles. This mismatch between land occupancy (de facto) and legal allocation (de jure) was also noted by Gaveau et al., 2017 in Sumatra who noted unregistered medium-sized landowners operate like companies in terms of their approach to oil palm development, but without formal company status. Missing young plantations cannot explain the large difference we notice in Indonesia between our planted area estimate and FOA harvested

385 area because expansion has gone down in recent years (Gaveau et al., 2019). In important producing regions (Riau, Sumatra), only 15% of all agricultural land parcels have a national-level registration and 26% of all oil palm plantations were only registered at the village level (Meijaard et al., 2018). Unregistered plantations explain why we found more plantations than FAO FAOSTAT.

In Malaysia, we also found a discrepancy between what is reported by the government and our data. Malaysia reports that

390 smallholder farms covered about 17% of the total area of oil palm cultivation in this country in 2018 (Senawi et al., 2019) as opposed to 21.7% identified in our dataset. The difference may relate to types of smallholders, with "organized smallholders" (as opposed to independent) operating in schemes that look like industrial-scale operation on imagery. Discrepancies between this study's findings and those of various governments on the ratio between smallholder and industrial scale oil palm could result from underestimations by authorities as identified by Oon and colleagues (2019. As

395 with Indonesia, it indicates how difficult it is to accurately map smallholder oil palm because of the heterogeneous characteristics of this land use, the lack of legal registration of smallholder lands, and potentially vested interests of running large-scale operations under small-holder type licenses (Supplementary figure 8).

5 Code availability

The code that generates the Sentinel-1 and Sentinel-2 composites can be found at:

400 https://github.com/adriadescals/oil_palm_global

6 Data availability

The dataset presented in this study is freely available for download at https://doi.org/10.5281/zenodo.3884602 (Descals et al., 2020). The dataset contains 622 100x100 km tiles, covering areas where oil palm plantations were detected. The file 'grid.shp' contains the grid that covers the potential distribution of oil palm. The file 'grid_withOP.shp' shows the 100x100

405 grid squares with presence of oil palm plantations. The classified images ('oil_palm_map' folder, in geotiff format) are the output of the convolutional neural network based on Sentinel-1 and Sentinel-2 half-year composites. The images have a spatial resolution of 10 meters and contain three classes: [1] Industrial closed-canopy oil palm plantations, [2] Smallholder

closed-canopy oil palm plantations, and [3] other land covers/uses that are not closed canopy oil palm. The file '*Validation_points_GlobalOilPalmLayer_2019.shp*' includes the 13,252 points that were used to validate the product. Each

410   point includes the attribute 'Class', which is the class assigned by visual interpretation, and the attribute 'predClass, which reflects the predicted class. The values of the 'Class' attribute are [0] other land covers/uses that are not closed canopy oil palm, [1] Industrial closed-canopy oil palm plantations, [2] Smallholder closed-canopy oil palm plantations. The 'predClass' values are identical to the 'Class' values.

The data can be visualized online at the BIOPAMA application portal: https://apps.biopama.org/oilpalm/. The BIOPAMA

415   application portal also includes the probability layer, which shows the probability (from 0 to 100) that a pixel is closed canopy oil palm plantation.

The Sentinel-1 SAR GRD and Sentinel-2 Level 2A used in this study are available at https://scihub.copernicus.eu/ and can be retrieved in Google Earth Engine (see Code availability section).

7 Conclusions

420   This study presents the first global map of oil palm plantations, for year 2019, derived from remotely-sensed data with a spatial resolution of 10 meters. We classified Sentinel-1 and Sentinel-2 data into a map that discriminates between smallholders and industrial oil palm plantations. We obtained high accuracies, with user's and consumer's accuracy generally above 80%, thanks to the use of cutting-edge deep learning algorithms. The method is deployable and can generate yearly maps for oil palm monitoring in a cloud processing environment and based on freely available satellite imagery.

425   Our global oil palm map makes an important contribution to palm oil debate. It will be useful to solve or at least clarify a range of social and environmental debates. We know that oil palm plantations are a major cause of deforestation in Indonesia and Malaysia (Austin et al., 2019; Gaveau et al., 2019), but the share of oil palm driven deforestation to global tropical forest loss is not known. This map will help to inform the debate on oil palm driven deforestation globally. Forest clearing for oil palm is associated with negative socio-economic impacts on forest-dependent communities (Santika et al., 2019). This map

430   validates a novel approach to mapping where oil palm is grown by smallholders who generate direct income or consumption from their own plantations, as opposed to industrial-scale oil palm (or industrial-scale plantings disguised as smallholder) where plantations provide labour opportunity but profits primarily attribute to company owners and the government (through taxes). The data can thus guide better planning for maximizing socio-economic benefits from oil palm. The global oil palm layer also assists in the discussion about environmental impacts of oil palm, including on biodiversity (Fitzherbert et al.,

435   2008; Meijaard et al., 2018) and regional climate (McAlpine et al., 2018). These negative impacts are real but need to be considered in the light of meeting the global demand for vegetable oil through optimal allocation of land not just to oil palm, but to all major oil-producing crops. This requires high-resolution spatial data for all oil seed crops (Meijaard et al., 2020), so

that informed decisions can be made about land use based on yield differences, past environmental and social impacts of different crops and the different characteristics of oils from different crops and their particular end uses. Finally, and relevant

440 to the current COVID-19 pandemic, our global map can help localize areas where zoonotic diseases can originate from, especially in areas where oil palm expansion was associated with recent deforestation. Such insights are essential for the health of people and the economy (Wardeh et al., 2020).

Supplement. Supplementary material related to this article is available online at: https://doi.org/10.5194/essd-XX-XXXX-
445 XXXX-supplement.

Author contributions. The concept for this work originated by ZS during scientific project discussions with SW, EM and SP for a goal of providing the scientific and policy making community with up to date and repeatable monitoring capabilities of oil palm plantations. AD and ZS designed the study, AD collected the training data, and AD and SW collected the
450 validation points. AD implemented the data processing workflow. AD, ZS, SW, EM, DG and SP were involved in the analysis and the writing of the manuscript, and AD generated the figures and tables.

Competing interests. The authors declare that they have no conflict of interest.

455 **Disclaimer.** All features and data are provided "as is" with no warranties of any kind. The views expressed are purely those of the writers and may not in any circumstance be regarded as stating an official position of the European Commission.

Review statement. This paper was edited by Dr. David Carlson and reviewed by XX anonymous referees.

470 **References**

Austin, K. G., Schwantes, A., Gu, Y., & Kasibhatla, P. S. (2019). What causes deforestation in Indonesia? *Environmental Research Letters*, *14*(2), 024007.

Bronkhorst, E., Cavallo, E., van Dorth tot Medler, M., Klinghammer, S., Smit, H. H., Gijsenbergh, A., & van der Laan, C. (2017). *Current practices and innovations in smallholder palm oil finance in Indonesia and Malaysia: Long-term financing solutions to promote sustainable supply chains* (Vol. 177). CIFOR.

Byerlee, D., Falcon, W. P., & Naylor, R. (2017). *The tropical oil crop revolution: Food, feed, fuel, and forests*. Oxford University Press.

Chen, L.-C., Zhu, Y., Papandreou, G., Schroff, F., & Adam, H. (2018). Encoder-decoder with atrous separable convolution for semantic image segmentation. *Proceedings of the European Conference on Computer Vision (ECCV)*, 801–818.

Descals, A., Szantoi, Z., Meijaard, E., Sutikno, H., Rindanata, G., & Wich, S. (2019). Oil Palm (Elaeis guineensis) Mapping with Details: Smallholder versus Industrial Plantations and their Extent in Riau, Sumatra. *Remote Sensing*, *11*(21), 2590.

Descals, A., Wich, S., Meijaard, E., Gaveau, D., Peedell, S., & Szantoi, Z. (2020). *High resolution global industrial and smallholder oil palm map for 2019*. Zenodo. https://doi.org/10.5281/zenodo.3884602

Fitzherbert, E. B., Struebig, M. J., Morel, A., Danielsen, F., Brühl, C. A., Donald, P. F., & Phalan, B. (2008). How will oil palm expansion affect biodiversity? *Trends in Ecology & Evolution*, *23*(10), 538–545.

Gaveau, D. L., Locatelli, B., Descals, A., Meijaard, E., & Sheil, D. (n.d.). *Rise and fall of oil palm and pulpwood plantations in Indonesia (2000-2019)*.

Gaveau, D. L., Locatelli, B., Salim, M. A., Yaen, H., Pacheco, P., & Sheil, D. (2019). Rise and fall of forest loss and industrial plantations in Borneo (2000–2017). *Conservation Letters*, *12*(3), e12622.

Gaveau, D. L., Pirard, R., Salim, M. A., Tonoto, P., Yaen, H., Parks, S. A., & Carmenta, R. (2017). Overlapping land claims limit the use of satellites to monitor no-deforestation commitments and no-burning compliance. *Conservation Letters*, *10*(2), 257–264.

Glenday, S., & Gary, P. (2015). Indonesian oil palm smallholder farmers: A typology of organizational models, needs, and investment opportunities. *Bogor (ID): Daemeter Consulting*.

Hijmans, R. J., Cameron, S. E., Parra, J. L., Jones, P. G., & Jarvis, A. (2005). Very high resolution interpolated climate

surfaces for global land areas. *International Journal of Climatology: A Journal of the Royal Meteorological Society*,

25(15), 1965–1978.

IFPRI. (2019). *Global Spatially-Disaggregated Crop Production Statistics Data for 2010, Version 1.0*. Harvard Dataverse.

500   Jelsma, I., Schoneveld, G. C., Zoomers, A., & Van Westen, A. (2017). Unpacking Indonesia's independent oil palm

smallholders: An actor-disaggregated approach to identifying environmental and social performance challenges.

Land Use Policy, *69*, 281–297.

Koh, L. P., Miettinen, J., Liew, S. C., & Ghazoul, J. (2011). Remotely sensed evidence of tropical peatland conversion to oil

palm. *Proceedings of the National Academy of Sciences*, *108*(12), 5127–5132.

505   https://doi.org/10.1073/pnas.1018776108

LeCun, Y., Bengio, Y., & Hinton, G. (2015). Deep learning. *Nature*, *521*(7553), 436–444.

Lee, J. S. H., Wich, S., Widayati, A., & Koh, L. P. (2016). Detecting industrial oil palm plantations on Landsat images with

Google Earth Engine. *Remote Sensing Applications: Society and Environment*, *4*, 219–224.

Li, W., Fu, H., Yu, L., & Cracknell, A. (2017). Deep learning based oil palm tree detection and counting for high-resolution

510   remote sensing images. *Remote Sensing*, *9*(1), 22.

Ma, L., Liu, Y., Zhang, X., Ye, Y., Yin, G., & Johnson, B. A. (2019). Deep learning in remote sensing applications: A meta-

analysis and review. *ISPRS Journal of Photogrammetry and Remote Sensing*, *152*, 166–177.

McAlpine, C. A., Johnson, A., Salazar, A., Syktus, J., Wilson, K., Meijaard, E., Seabrook, L., Dargusch, P., Nordin, H., &

Sheil, D. (2018). Forest loss and Borneo's climate. *Environmental Research Letters*, *13*(4), 044009.

515   Meijaard, E, Garcia-Ulloa, J., Sheil, D., Wich, S., Carlson, K., Juffe-Bignoli, D., & Brooks, T. (2018). *Oil palm and

biodiversity: A situation analysis by the IUCN Oil Palm Task Force*.

Meijaard, Erik, Abrams, J., Juffe-Bignoli, D., Voigt, M., & Sheil, D. (2020). Coconut oil, conservation and the conscientious

consumer. *CURRENT-BIOLOGY-D-20-00608*.

Meijaard, Erik, & Sheil, D. (2019). The Moral Minefield of Ethical Oil Palm and Sustainable Development. *Frontiers in

520   Forests and Global Change*, *2*. https://doi.org/10.3389/ffgc.2019.00022

Miettinen, J., & Liew, S. C. (2011). Separability of insular Southeast Asian woody plantation species in the 50 m resolution ALOS PALSAR mosaic product. *Remote Sensing Letters*, *2*(4), 299–307.

Nomura, K., Mitchard, E. T., Patenaude, G., Bastide, J., Oswald, P., & Nwe, T. (2019). Oil palm concessions in southern Myanmar consist mostly of unconverted forest. *Scientific Reports*, *9*(1), 1–9.

525   OECD. (2018). *OECD-FAO agricultural outlook 2018-2027*. OECD Publishing.

Oon, A., Ngo, K. D., Azhar, R., Ashton-Butt, A., Lechner, A. M., & Azhar, B. (2019). Assessment of ALOS-2 PALSAR-2L-band and Sentinel-1 C-band SAR backscatter for discriminating between large-scale oil palm plantations and smallholdings on tropical peatlands. *Remote Sensing Applications: Society and Environment*, *13*, 183–190.

Paoli, G. D., Gillespie, P., Wells, P. L., Hovani, L., Sileuw, A., Franklin, N., & Schweithelm, J. (2013). Oil palm in

530   Indonesia: Governance, decision making and implications for sustainable development. *The Nature Conservancy, Jakarta, Indonesia*.

Pirker, J., Mosnier, A., Kraxner, F., Havlík, P., & Obersteiner, M. (2016). What are the limits to oil palm expansion? *Global Environmental Change*, *40*, 73–81.

Sandler, M., Howard, A., Zhu, M., Zhmoginov, A., & Chen, L.-C. (2018). Mobilenetv2: Inverted residuals and linear

535   bottlenecks. *Proceedings of the IEEE Conference on Computer Vision and Pattern Recognition*, 4510–4520.

Santika, T., Wilson, K. A., Budiharta, S., Kusworo, A., Meijaard, E., Law, E. A., Friedman, R., Hutabarat, J. A., Indrawan, T. P., St. John, F. A., & others. (2019). Heterogeneous impacts of community forestry on forest conservation and poverty alleviation: Evidence from Indonesia. *People and Nature*, *1*(2), 204–219.

Senawi, R., Rahman, N. K., Mansor, N., & Kuntom, A. (2019). TRANSFORMATION OF OIL PALM INDEPENDENT

540   SMALLHOLDERS THROUGH MALAYSIAN SUSTAINABLE PALM OIL. *Journal of Oil Palm Research*, *31*(3), 496–507.

Shaharum, N. S. N., Shafri, H. Z. M., Ghani, W. A. W. A. K., Samsatli, S., Al-Habshi, M. M. A., & Yusuf, B. (2020). Oil palm mapping over Peninsular Malaysia using Google Earth Engine and machine learning algorithms. *Remote Sensing Applications: Society and Environment*, 100287.

545   Strona, G., Stringer, S. D., Vieilledent, G., Szantoi, Z., Garcia-Ulloa, J., & Wich, S. A. (2018). Small room for compromise between oil palm cultivation and primate conservation in Africa. *Proceedings of the National Academy of Sciences*, *115*(35), 8811–8816.

Wardeh, M., Sharkey, K. J., & Baylis, M. (2020). Integration of shared-pathogen networks and machine learning reveals the key aspects of zoonoses and predicts mammalian reservoirs. *Proceedings of the Royal Society B*, *287*(1920),
550   20192882.

Wich, S. A., Garcia-Ulloa, J., Kühl, H. S., Humle, T., Lee, J. S., & Koh, L. P. (2014). Will oil palm's homecoming spell doom for Africa's great apes? *Current Biology*, *24*(14), 1659–1663.

Woittiez, L. S., van Wijk, M. T., Slingerland, M., van Noordwijk, M., & Giller, K. E. (2017). Yield gaps in oil palm: A quantitative review of contributing factors. *European Journal of Agronomy*, *83*, 57–77.

555   Xu, Y., Yu, L., Li, W., Ciais, P., Cheng, Y., & Gong, P. (2020). Annual oil palm plantation maps in Malaysia and Indonesia from 2001 to 2016. *Earth System Science Data*, *12*(2), 847–847.